Electrical properties of SnO₂ ceramic varistors withstanding high current pulses

Glot A. B. *
Universidad Tecnológica de la Mixteca
Huajuapan de León, Oaxaca, 69000, México

Lu Z. Y., Zhou Z. Y.
South China University of Technology
Guangzhou, 510640, China

Ivon A. I.
Dniepropetrovsk National University
Dniepropetrovsk, 49010, Ukraine

Electrical properties of new dense SnO₂-CoO-Nb₂O₅-Cr₂O₃-Y₂O₃ varistor ceramics are studied. Current-voltage characteristics in the wide range from 10^{-11} to about $3.3 \cdot 10^3$ A·cm⁻² contain three regions. At low currents linear (Ohmic) region is found. Highly nonlinear region with the nonlinearity coefficient of about 50 at 1 mA·cm⁻² is observed between 10^{-6} and 1 A·cm⁻². At higher currents the upturn region is revealed. In this region the slope of current-voltage characteristic in the double logarithmic scale is decreased. The increase in dc current on time at fixed voltage and the hysteresis in the ac current-voltage characteristic are observed. These features can be related to Joule heating or electronic processes. However, after the high-current pulses only minor changes at low current are found. This indicates that studied ceramics withstand high-current overloads. This fact can be attributed to the formation of quite identical electrically-active grain boundaries throughout a sample. The grain resistivities $\rho_G \cong 1.2 - 2.2 \ Ohm \cdot cm$ estimated from high-current pulse data are the lowest known up to now for SnO₂ varistors.

Keywords: Grain boundary; Non-Ohmic conduction; Potential barrier; Pulse stability; Tin dioxide; Varistor

1. Introduction

Metal oxide varistor (a sample of suitable ceramic material with two electrodes) is semiconductor device with superlinear and symmetric dependence of current I on voltage U. Usually current-voltage ($I(U)$) characteristic of varistor is approximated by the empiric expression (written for the current density J and the electric field E):

$$J = BE^{\beta}, \tag{1}$$

where B and β are constants. The degree of the nonlinearity is frequently estimated by the empiric nonlinearity coefficient:

$$\beta = \frac{E}{J}\frac{dJ}{dE} = \frac{d(\log J)}{d(\log E)}. \tag{2}$$

The nonlinearity coefficient β and the electric field strength E_1 calculated at fixed current density (usually at 1 mA cm⁻²) are used as the main empiric parameters of varistor.
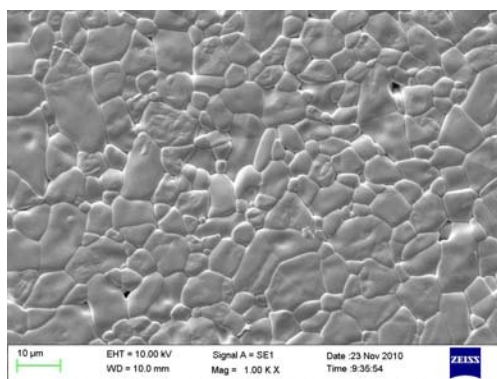
At present, ZnO-based ceramic varistors with $\beta > 20$ [1] are widely used for protection of electronic and electrical equipment against transient surges [2-4]. Fairly strong non-Ohmic conduction was observed in SnO₂-based ceramics [5-7] and now SnO₂ varistor ceramics are intensively studied [8-13].
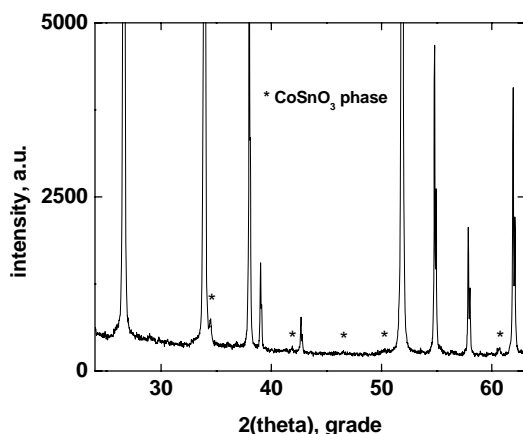
The varistor effect in ZnO-based and in SnO₂-based ceramics is electronic in its nature: it is related to the transport of the majority carriers (electrons) controlled by the grain-boundary potential barriers formed during sintering in oxidizing atmosphere [2-13]. The varistor effect in ZnO and in SnO₂ ceramics can be explained as a sharp decrease in the barrier height due to a participation of minority carriers (holes) appeared as a consequence of threshold impact ionization or threshold tunneling (Zener effect) [14-19].

Frequently in the literature only dc $J(E)$ characteristics (below about 10 mA·cm⁻²) are discussed. Meanwhile varistors in real circuits works in dc (or ac) and pulse modes. Therefore, $J(E)$ characteristics obtained in a wide current range from nA to kA give rather more complete characterization of ceramic ZnO or SnO₂ varistor [1-4,11,17,20-25].
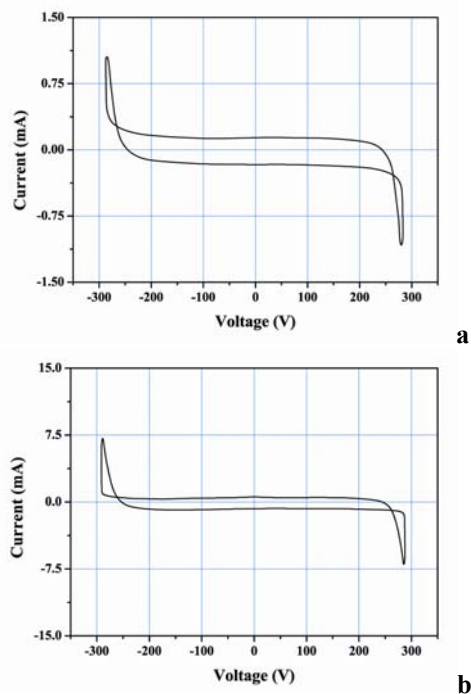
Current flow in varistor ceramics can be accompanied by the Joule heating if dc or ac current is too high or heat-sink cooling is not enough. Therefore, sometimes Joule heating can undesirably modify electrical characteristics. But usually researchers do not pay attention to possible

* On leave from Dniepropetrovsk National University Dniepropetrovsk, 49010, Ukraine (alexglot@mixteco.utm.mx, alexglot@mail.ru)

Figure 1. SEM micrograph of the surface of SnO$_2$-CoO-Nb$_2$O$_5$-Cr$_2$O$_3$-Y$_2$O$_3$ ceramics.

Figure 2. XRD pattern for SnO$_2$-CoO-Nb$_2$O$_5$-Cr$_2$O$_3$-Y$_2$O$_3$ ceramic material. The peak positions for CoSnO$_3$ phase are marked with asterisk.

Figure 3. Oscillograms of I(U) characteristics of SnO$_2$-CoO-Nb$_2$O$_5$-Cr$_2$O$_3$-Y$_2$O$_3$ ceramic varistor (50 Hz). In "a" and "b" I(U) characteristics of the same sample but with different vertical scale are shown.

contribution of Joule effect. The Joule self heating can be especially important in SnO$_2$ varistor ceramics where some porosity is observed and due to that rather poor grain-to-grain contacts can be assumed [26] even if ceramics were obtained by liquid-phase sintering [27]. It was reported [26] that Joule heating is responsible for current rise on time especially in the range of relatively high dc currents where actually the nonlinearity of $I(U)$ dependence is quite high. The Joule self heating can be responsible for the irreversible electro-thermal breakdown of SnO$_2$ ceramic varistors during high-current pulse tests [27]. It can be due to the inhomogeneous distribution of current over cross-section of a sample. However, in some laboratories high-current pulse tests of SnO$_2$ ceramic varistors gave promising results showing that such samples can withstand high-current pulses [23-25]. It would be interesting to study such SnO$_2$ ceramic varistors and understand the role of the Joule self heating in their low-current and high-current properties.

Therefore, in this paper we study dc and ac electrical properties of SnO$_2$-based varistor ceramics in a system SnO$_2$-CoO-Nb$_2$O$_5$-Cr$_2$O$_3$-Y$_2$O$_3$ in the wide current range from about 10^{-11} up to 3.3 kA·cm^{-2} with the attention to possible manifestation of the Joule self heating in electrical characteristics.

2. Experimental details

Tin dioxide based SnO$_2$-CoO-Nb$_2$O$_5$-Cr$_2$O$_3$-Y$_2$O$_3$ ceramics were obtained according to a recently reported procedure [25]. The composition was (mol.%) 97.35 SnO$_2$, 2.5 CoO, 0.05Nb$_2$O$_5$, 0.05Cr$_2$O$_3$ and 0.05Y$_2$O$_3$. SnO$_2$ powder (purity of 99.5%) was blended with additives and ball milled with distilled water. PVA solution was used for granulation. The granulated powder was pressed into discs at a pressure of about 150 MPa. After removing of the organic binder, the discs were placed in a covered aluminum crucible and sintered at 1300 C for 2 hours in air. Silver electrodes were obtained at 600 C. The sizes of studied samples were: thickness 1 mm and diameter (of electrodes) 12 mm.

For materials characterization scanning electron microscopy (SEM) (FEI-Quanta 200) and X-ray diffraction (XRD) (Philips X´pert MPD) were used. Dc measurements were conducted by using source-measure unit Keithley-237. Ac (50 Hz) current-voltage characteristics were obtained using TR4401 oscilloscope. Original oscillogramms were treated using "G3 data" program to improve their quality. The dependences of small-signal capacitance and ac conductance at frequency 1 kHz on time at different dc voltages were obtained using precision LRC meter 7600-B (QuadTech) and source-measure unit Keithley-6487.

Pulse properties of varistors were tested using 8/20 μs current pulses generated at capacitance discharge over circuit containing tested varistor. For $8/20$ μs pulse test, the discs with electrodes were soldered with tinned copper leads and coated with epoxy resin, with the aim to avoid

electrical breakdown of air at the lateral parts of a sample at high applied voltage. The current and voltage waveforms were recorded using storage oscilloscope. Peak current and voltage values were used to plot $I(U)$ characteristic.

3. Results and discussion

Samples of SnO_2-CoO-Nb_2O_5-Cr_2O_3-Y_2O_3 ceramics are quite dense (Fig.1). The grain size distribution is rather wide. There are relatively large SnO_2 grains of about 10 μm and smaller SnO_2 grains of about 2 μm. The inclusions of other phases are not seen in Fig.1, though, XRD confirms that this material contains, additionally to the main SnO_2 crystalline phase, small quantity of $CoSnO_3$ phase (Fig.2). Fairly good sintered material (Fig.1) can have relatively high cross-section of grain boundaries what is important for high current transport.

It is useful to see the oscillogram of the current-voltage characteristic of a nonlinear device. Additionally, the Joule heating can cause some inertia in $I(U)$ behavior which can be seen in its oscillogram [12]. With this aim current-voltage characteristics were studied at ac voltage (50 Hz). In Fig.3 the oscillograms of $I(U)$ characteristics of SnO_2-CoO-Nb_2O_5-Cr_2O_3-Y_2O_3 ceramic varistor are presented.

In Fig.3,b maximal current is about one decade higher than in Fig.3,a. At low voltages some vertical bifurcation is related to capacitive current because this bifurcation is higher in the samples with higher low-voltage capacitance. At high voltages the hysteresis in $I(U)$ characteristic is seen (Fig.3,a,b). The increase in current with voltage is quite sharp. Though, the decrease in current with voltage is less sharp due to some micro regions in the sample are still sufficiently heated. In Fig.3,b the transition to highly nonlinear region is clearly seen as vertical current jump but current decrease give more flattened curve. Observed hysteresis in the highly nonlinear part of $I(U)$ characteristic is due probably to the Joule heating, though, it is possible that the observed behavior may be caused by some electronic processes in the barrier region.

Similar hysteresis was found in other SnO_2-based varistors [12,26]. In ZnO-based varistors such hysteresis is lower or visibly absent [12,26]. Observed hysteresis can be probably related to phenomenon of "inductive-type" behavior of current (increase in current on time at rectangular voltage pulse) observed in ZnO varistors [1,28] and in SnO_2 varistors (our observations) and phenomenon of "negative small-signal capacitance" in ZnO varistors [16,29,30] and in SnO_2 varistors [6,19] or can probably strengthen such phenomena.

Application of low dc voltage causes gradual decrease of current on time and during some short time current becomes fairly stable. Therefore, for the study of nearly steady state current-voltage characteristic voltage was applied during 120 s and current was recorded at the end of this period. Then higher voltage was applied stepwise and current was recorded again and etc. Obtained data are shown in Fig.4. It is seen that at low voltages current is
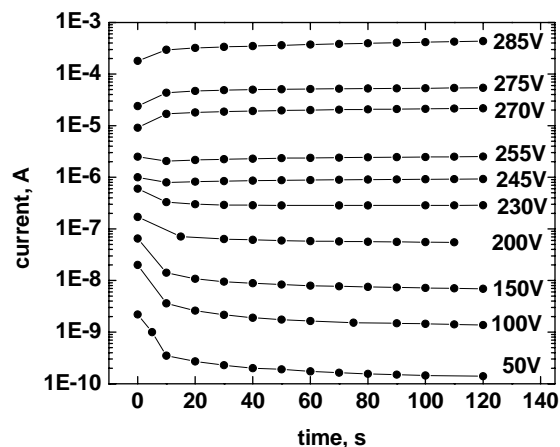

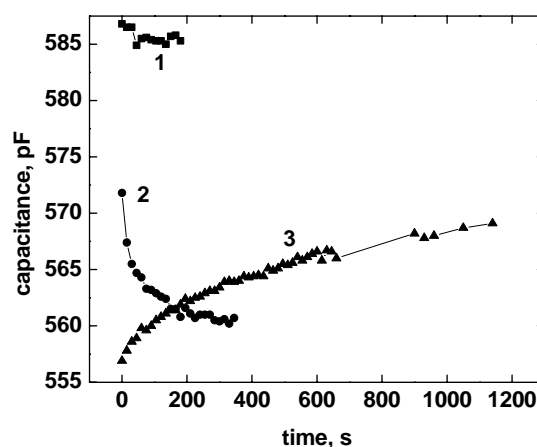**Figure 4.** Time dependences of current at fixed dc voltages.

Figure 5. Time dependences of capacitance at zero dc bias (1), at 100 V dc bias (2) and at zero dc bias after the application 100V (3).

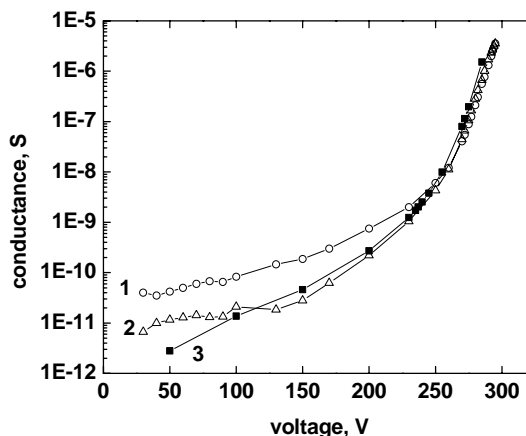**Figure 6.** Current-voltage characteristics of SnO_2-CoO-Nb_2O_5-Cr_2O_3-Y_2O_3 varistor ceramics. Data obtained at increase (1) and decrease (2) of voltage applied during 2-3 s. At curve 3 current values were measured if voltage was applied during 120 s at each point.

Table 1. Electrical parameters of SnO_2-CoO-Nb_2O_5-Cr_2O_3-Y_2O_3 varistor (thickness 1 mm, diameter of electrodes 12 mm, with copper leads, coated with epoxy resin).

U_{1mA} (V)	β	$0.75 \cdot U_{1mA}$ $I_L(\mu A)$	C_{1kHz} (pF)
294	53	0.35	585

U_{1mA}: voltage at 1 mA; β: nonlinearity coefficient at 1 mA; I_L: leakage current (current at 0.75 $U_{1\,mA}$); C_{1kHz}: capacitance at 1 kHz.

decreased on time but at higher voltages the increase in current on time is observed (Fig.4).

In SnO_2-based ceramics electrical conduction is controlled by potential barriers formed at the grain boundaries during sintering in oxidizing atmosphere [5-13]. Electrons are captured at the surface oxygen centers and positive charge of ionized donors in the depletion layers of the adjacent grains are screened mentioned negative surface charge. Therefore, observed decay of current on time if voltage is applied, can be related to a breach of dynamic equilibrium between capture and emission of majority carriers (electrons) at the grain boundary. As a result capture is dominated over emission, the barrier height is increased and current is decreased.

For the confirmation of such picture the dependence of capacitance on time was measured (Fig.5). Actually, capacitance at relatively high frequency about 1 kHz gives some information about the width of the depletion regions. It is seen from Fig.5 that capacitance is decreased on time and on dc bias. Grain-boundary capacitance can be assumed as forward-biased and reverse-biased parts of capacitance connected in series. Then decreasing of capacitance on time is due to the capture of electrons at the grain-boundary states. Negative interface charge is increased and, therefore, depletion layers in adjacent grains become wider. If dc bias is taken off, than emission is dominated over capture, negative interface charge is decreased on absolute value, depletion layers become narrower and capacitance is increased on time (curve 3 in Fig.5). The decrease of capacitance on dc bias means widening of reverse-biased depletion layer. Therefore, observed decrease in capacitance on time and dc bias confirms discussed earlier decrease in dc current on time (Fig.4). Ac conductance data demonstrate similar behavior but the scattering in ac conductance is stronger than in the capacitance. These results give the basis for discussing the grain-boundary controlled conduction in the studied SnO_2-based varistor ceramics.
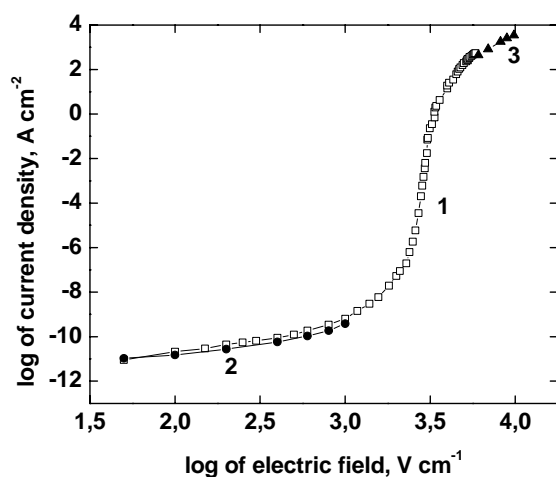
The current rise on time observed at higher voltages (Fig.4) can be explained by Joule self heating. However, processes probably are more complex than simple Joule heating because, on the one hand, Joule heating leads to some increase in temperature of grain boundaries which causes higher heat transfer from the grain boundary to adjacent grains and from tested sample to the sample holder. On the other hand, increase in current on time at higher voltages can be due to the gradual establishment of

new dynamic equilibrium between capture and emission of majority carriers at the grain boundary. In any case as a result of thermal and electronic processes the equilibrium current can be reached because the slope dI/dt of this dependence is decreased on time (Fig.4). Observed increase in current on time at higher voltages with a tendency to stabilization correlates with the behavior of current on time in SnO_2-CoO-Nb_2O_5-Cr_2O_3 varistor ceramics at accelerated ageing when current flowed across a sample during long time about 170 hours [31].

Due to the observed changes in current on time at fixed voltages (Fig.4) some variation in current-voltage characteristic depending on a rate of voltage change is expected. In Fig.6 current-voltage characteristics of the same sample were recorded if voltage was changed relatively quickly (each 2-3 s) or slowly (each 120 s). Two features are found. At low voltages some hysteresis is observed (curves 1 and 2 in Fig.6): I(U) characteristic obtained at decreasing voltage is situated slightly below than I(U) dependence obtained at increasing voltage due to some additional electronic charge was captured at the grain boundaries. At high voltages (in the highly nonlinear region) longer application of voltage causes some increase in current (see Fig.4), therefore, current-voltage characteristic exhibit some higher slope. This means that the nonlinearity coefficient can be overestimated due to possible Joule heating. Probably, the values of the nonlinearity coefficient reported in the literature sometimes can be overestimated due to this reason. But numerical values of parameters can be useful for approximate comparison of different materials. With this purpose in Table 1 basic electrical parameters of one of the studied sample are shown.

Taking into account observed influence of Joule heating on dc and ac current it can be assumed that studied SnO_2-based varistors can be strongly degraded or even be destroyed at pulses of high current. However, according to published data these SnO_2-based varistors are able to withstand high-current pulses [25]. Therefore, it would be interesting to test by high-current pulses exactly those samples for which data of Fig.3-6 were obtained.

In Fig.7 (curve 1) J(E) characteristic of SnO_2-CoO-Nb_2O_5-Cr_2O_3-Y_2O_3 ceramic varistor obtained in dc regime (below about 1 mA·cm^{-2}) and in pulse regime (above about 1 mA·cm^{-2}) is shown. It is important to mention that just after high-current pulse measurements (curve 1) dc J(E) characteristic (curve 2) is situated just slightly below the
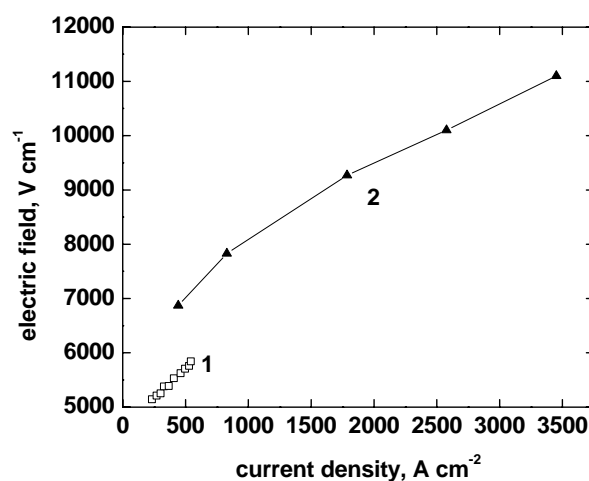
Figure 7. J(E) characteristic of SnO_2-CoO-Nb_2O_5-Cr_2O_3-Y_2O_3 ceramic varistor obtained in dc (1,2) and pulse (1,3) regime. Pulse tests were performed on similar samples but using different equipment. Curve 2 gives dc J(E) characteristic after the pulse test presented by curve 1.

Figure 8. Pulse E(J) characteristics (see Fig.7) presented in linear scale. Curve 1 is formed by several high-current points taken from curve 1 in Fig.7. Curve 2 presents the same data as curve 3 in Fig.7.

initial one (curve 1). It means that no undesirable degradation (increase in low-field conductivity) is occurred. Observed slight decrease in conductivity (Fig.7, curve 2) can be explained by the residual filling of grain-boundary states. Using other pulse equipment some higher current density of about 3.3 kA·cm^{-2} was reached for other samples of the same preparation method and the same diameter of electrodes (12 mm) (Fig.7, curve 3). Both pulse data (curve 1 and curve 3 in Fig.7) are combined satisfactorily in logarithmic scale.

At the current-voltage characteristic of SnO_2-based varistor obtained in a wide current range three regions with gradual transitions between them can be distinguished (Fig.7, curves 1 and 3): linear (Ohmic) region at low currents, highly nonlinear region from about 10^{-6} A·cm^{-2} to about 1 A·cm^{-2} and upturn region where the slope of J(E) characteristic in the double logarithmic scale again becomes low. The highly nonlinear region in J(E) characteristic is attributed to the decrease in the barrier height of the grain-boundary potential barriers. The appearance of the upturn region in J(E) characteristic is related to increasing of voltage drop at SnO_2 grains. The higher the current the higher voltage drop at SnO_2 grains. The voltage drop at SnO_2 grains is added to the voltage drop at the grain boundaries. It is necessary to stress that at lower currents (in the highly nonlinear region) the whole voltage drop is at the grain boundaries and the voltage drop at SnO_2 grains is negligible, though at higher currents the voltage drop at the sample consist of two parts: the voltage drop at the grain boundaries and the voltage drop at the grains.

It is seen that in the upturn region current is substantially limited by the grain resistance. Therefore, the grain resistivity is very important varistor parameter. It is possible to estimate the grain resistivity value using upturn region of J(E) characteristic.

If current is quite high (in the upturn region) and significant part of voltage is dropped at grains, then J(E)

characteristic becomes approximately linear and the grain resistivity ρ_G can be estimated according [17,20-21]:

$$\rho_G \cong \Delta E / \Delta J , \tag{3}$$

where ΔE is the increment of electric field and ΔJ is respective increment of current density in the upturn region of J(E) characteristic.

In Fig.8 experimental data of Fig.7 are shown in linear scale. Curve 1 in Fig.8 reflects several high-current points taken from curve 1 in Fig.7. Curve 2 in Fig.8 presents the same data as curve 3 in Fig.7. Curve 1 in Fig.8 can be approximated by the right line and according to Eq. (3) we have: $\rho_G \cong 2.2$ *Ohm·cm*. Curve 2 in Fig.8 is slightly displaced from the curve 1 due to other sample (but of the same preparation method and the same diameter of electrodes) was used. Curve 2 in Fig.8 is related to wider J and E range. It is slightly nonlinear, however, some linear part at high currents can be selected. Respective estimation using Eq. (3) gives: $\rho_G \cong 1.2$ *Ohm·cm*. Obtained lower value of ρ_G corresponds some lower slope of curve 2 in Fig.8. Probably at lower current density (Fig.8, curve 1) contribution of voltage drop at the barrier region is more significant and, therefore, estimation is less exact. It means that the value $\rho_G \cong 1.2$ *Ohm·cm* is closer to reality.

Estimated values of the grain resistivity $\rho_G \cong 1.2 - 2.2$ *Ohm·cm* for the studied SnO_2-varistors are quite low. Earlier significantly higher values of the grain resistivity in other SnO_2-based ceramic varistors were reported. In SnO_2-ZnO-Bi_2O_3 varistors the grain resistivity is about 40 *Ohm·cm* [20]. In SnO_2-Co_3O_4-Nb_2O_5-Cr_2O_3-Bi_2O_3 varistors the value of about 4 *Ohm·cm* was estimated [32]. Extremely high grain resistivity of about $1 \cdot 10^3$ *Ohm·cm* was reported in SnO_2-CoO ceramics [11].

In SnO$_2$-Co$_3$O$_4$-Nb$_2$O$_5$-Cr$_2$O$_3$-CuO varistor ceramics the grain resistivity in the range $11-17$ $Ohm \cdot cm$ was found [27]. Therefore, estimated here values of the grain resistivity $\rho_G \cong 1.2-2.2$ $Ohm \cdot cm$ for SnO$_2$-CoO-Nb$_2$O$_5$-Cr$_2$O$_3$-Y$_2$O$_3$ ceramics are the lowest among published for SnO$_2$-based ceramic varistors. For ZnO varistors the grain resistivity is about $0.25-0.5$ $Ohm \cdot cm$ [20,21,33-35]. This means that SnO$_2$-CoO-Nb$_2$O$_5$-Cr$_2$O$_3$-Y$_2$O$_3$ varistor ceramics possess quite low grain resistivity closely approaching to the grain resistivity in ZnO varistor ceramics.

The addition of higher amount of CoO (2.5 mol.%) makes this ceramic material quite dense (Fig.1). Probably, the densification (due to CoO addition) and addition of Y$_2$O$_3$ promote more homogeneous creation of oxygen vacancies and more homogeneous distribution of Nb throughout a sample. The oxygen vacancies and Nb atoms can be donor impurities in tin dioxide [12,13]. More homogeneous distribution of donors in a sample can explain lower grain resistivity observed in the studied material. If the distribution of donors in a sample is not sufficiently homogeneous then the average grain resistivity is higher. Additionally, probably, Y$_2$O$_3$ in parallel to Cr$_2$O$_3$ helps in a formation of rather equal barriers at different grain boundaries in a sample. Therefore, at high current pulses a sample will behave homogeneously (more part of cross-section will be used), current will be higher at the same voltage, resistance is decreased and the grain resistivity is decreased as well.

Low-current electrical properties of SnO$_2$-CoO-Nb$_2$O$_5$-Cr$_2$O$_3$-Y$_2$O$_3$ varistor ceramics with quite high pulse stability studied here are sufficiently similar to low-current electrical properties of other ceramics [26] with significantly lower pulse stability. However, the only difference between both mentioned materials rather is in microstructure: according to SEM observations, studied here SnO$_2$-based varistor ceramics are better sintered materials with no visible porosity (Fig.1). Probably, more dense arrangement of grains promotes adequate dissipation of heat generated in the grain-boundary regions but the grain resistivity is very low and, therefore, heat generated in the grains themselves can be substantial only at quite high currents.

Conclusions

Current-voltage characteristics of new dense SnO$_2$-CoO-Nb$_2$O$_5$-Cr$_2$O$_3$-Y$_2$O$_3$ varistor ceramics are reproducible in the wide current range and, similarly to ZnO varistor ceramics, contain linear, highly nonlinear and upturn regions. Electrical conduction in the linear and highly nonlinear regions are controlled by the grain-boundary potential barriers with the barrier height strongly dependent on electric field. In the highly nonlinear region the nonlinearity coefficient is about 50-54. In the upturn region the slope of current-voltage characteristic in double logarithmic scale is decreased due to the non-zero grain

resistivity. The estimated grain resistivity $\rho_G \cong 1.2-2.2$ $Ohm \cdot cm$ is the lowest known up to now for SnO$_2$ varistors. It is surprising that samples exhibit the Joule self heating at relatively low dc currents but withstand high-current pulses. The absence of irreversible breakdown in such case can point out that throughout a sample quite identical electrically-active grain boundaries are formed. High nonlinearity combined with low pulse degradation and quite low grain resistivity certify that SnO$_2$-CoO-Nb$_2$O$_5$-Cr$_2$O$_3$-Y$_2$O$_3$ ceramics exhibit fairly reasonable varistor properties.

References

[1]. M. Matsuoka, Jap. J. Appl. Phys. **10**, 736 (1971).
[2]. T. K. Gupta, J. Am. Ceram. Soc. **73**, 1817 (1990).
[3]. D. R. Clarke, J.Am.Ceram.Soc. **82**, 485 (1999).
[4]. B. K. Avdeenko, A. B. Glot, A. I. Ivon, I. M. Chernenko and A. I. Schelokov, Inorg. Mater. **16**, 1059 (1980).
[5]. A. B. Glot and A. P. Zlobin, Inorganic Materials **25**, 274 (1989).
[6]. A. B. Glot, Yu. N. Proshkin, A. M. Nadzhafzade, in: Ceramics Today –Tomorrow´s Ceramics. Materials science monographs, vol. 66C, Ed. P. Vincenzini (Elsevier, 1991) p. 2171.
[7]. S. A. Pianaro, P. R. Bueno, E. Longo and J. A. Varela, J. Mater. Sci. Lett. **14** 692 (1995).
[8]. P. N. Santhosh, H. S. Potdar and S. K. Date, J. Mater. Res. **12**, 326 (1997).
[9]. R. Parra, M. A. Ponce, C. M. Aldao and M. S. Castro J. Eur. Ceram. Soc. **27,** 3907 (2007).
[10]. S. R. Dhage and V. Ravi, Appl. Phys. Lett. **83,** 4539 (2003).
[11]. R. Metz, D. Koumeir, J. Morel, J. Pansiot, M. Houabes and M. Hassanzadeh, J. Eur. Ceram. Soc. **28**, 829 (2008).
[12]. A. B. Glot, in: Ceramic Materials Research Trends, Ed. P. B. Lin (Nova Science Publishers, Inc., New York, 2007) p. 227.
[13]. P. R. Bueno, J. A. Varela and E. Longo, J. Eur. Ceram. Soc. **28,** 505(2008).
[14]. R. Einzinger, Appl. Surf. Sci. **3**, 390 (1979).
[15]. G. D. Mahan, L. M. Levinson and H. R. Philipp, J.Appl.Phys. 50, 2799(1979).
[16]. G. E. Pike, in: Grain Boundaries in Semiconductors, Eds. H. J. Leamy, G. E. Pike, C. H. Seager (North-Holland, New York, 1982) p. 369.
[17]. A. I. Ivon, A. B. Glot, I. M. Chernenko, in: Fourth Euro-Ceramics. V.5. Electroceramics, Ed. G. Gusmano and E. Traversa (Gruppo Editoriale Faenza Editrice, Faenza, Italy, 1995) p. 475.
[18]. A. B. Glot, J. Mater. Sci. **41**, 5709 (2006).
[19]. A. B. Glot, A. V. Gaponov and A. P. Sandoval-García, Phys. B: Condensed Matter, **405**, 705 (2010).
[20]. A. I. Ivon, A. B. Glot, A. V. Gaponov and S. V. Mazurik, Key Eng. Mater. **132**, 1289 (1997).
[21]. A. I. Ivon, Inorg. Mater., **36**, 1074(2000).
[22]. R. Metz, J. Morel, M. Houabes, J. Pansiot and M. Hassanzadeh, J. Mater. Sci. **42**, 10284 (2007).
[23]. M. A. Ramirez, W. Bassi, P. R. Bueno, E. Longo and J.A. Varela, J. Phys. D: Appl. Phys. **41**, 122002 (2008).
[24]. M. A. Ramirez, W. Bassi, R. Parra, P. R. Bueno, E. Longo and J.A. Varela, J. Am. Ceram. Soc. **91**, 2402 (2008).
[25]. Z.-Y. Lu, Z. Chen and J.-Q. Wu, J. Ceram. Soc. Japan **117**, 851 (2009).
[26]. A. B. Glot, A. N. Bondarchuk, A. I. Ivon, L. Fuentes, J. A. Aguilar-Martinez, M. I. Pech-Canul and N. Pineda-Aguilar, in:

XIX Int. Conf. on Extractive Metallurgy, Saltillo, Coah., Mexico (May 18-21, 2010, paper 52) p. 572.

[27]. A. V. Gaponov, A. B. Glot, A. I. Ivon and R. Bulpett, Phys. Chem. Solid State, **11**, 738 (2010).

[28]. K. Eda, J.Appl.Phys. **50**, 4436 (1979).

[29]. A. Ya. Karachentsev and Yu. N. Potashev, Electronnaya Tekhnika. Ser.5. Radiodetali i Radiocomponenty **4,** 37 (1973).

[30]. A. B. Glot, Advances in Varistor Technology. Ceramic Transactions, **3**, Ed. L. M. Levinson (Am. Ceram. Soc., Westerville, OH, 1989) p. 194.

[31]. M A Ramirez, M Cilense, P R Bueno, E Longo and J A Varela. J. Phys. D: Appl. Phys. **42**, 015503 (2009).

[32]. A. B. Glot and I. A. Skuratovsky, Mater. Chem. Phys. **99**, 487 (2006).

[33]. L. M. Levinson and H. R. Philipp, J.Appl.Phys. **47,** 3116 (1976).

[34]. W. G. Carlson and T. K. Gupta, J. Appl. Phys. **53,** 5746 (1982).

[35]. H. R. Philipp and L. M. Levinson, J. Appl. Phys. **47,** 1112 (1976).